The 6th Symp. on Accelerator Science and Technology, 1987, Tokyo, Japan (© Ionics, Tokyo, 1987)

NEUTRON PRODUCTION FROM HIGH ENERGY CHARGED PARTICLES

T. Nakamura
Cyclotron and Radioisotope Center, Tohoku University
Aoba, Aramaki, Sendai 980, Japan

Y. Uwamino
Institute for Nuclear Study, University of Tokyo
Midori-cho 3-2-1, Tanashi, Tokyo 188, Japan

ABSTRACT

The neutron yields and energy spectra produced by charged particle bombardment are evaluated. The neutron energy spectra are fitted to two or three Maxwellian-type components. The lowest energy component corresponds to the evaporation neutrons from a compound nucleus having a nuclear temperature independent of the neutron emission angle and the higher two components to the pre-equilibrium neutron emission having a nuclear temperature depending on the angle.

INTRODUCTION

The information on secondary neutron production, such as energy spectrum, angular distribution and total neutron yield, for various projectile and target combinations is quite important for the shielding design of high energy accelerator facilities, since these neutrons become the predominant radiation source. Many works have been done on secondary neutron production from thick targets bombarded by charged particles, as is summarized in ref. (1). The data of neutron yields produced by projectiles except proton are still very scarce. A simple empirical formula predicting total neutron yield and its angular distribution has been introduced[2] from the rather dispersed and incomplete experimental data and some theoretical results in the published papers. For neutron energy spectra from thick targets, our work[3),4)] is the only one on their analysis connected with the mechanism of producing neutrons from nucleon-nucleus and nucleus-nucleus collisions, except for the neutron spectrum analysis on the basis of the Serber model for deuteron stripping [5),6)].

PHENOMENOLOGICAL HYBRID ANALYSIS OF NEUTRON ENERGYCTRA

It can be considered that the energy spectrum of neutrons produced by light-mass heavy-ion bombardment is composed of the following four components:

1) Evaporation spectrum in the low energy region corresponding to neutron emission from an equilibrium state.
2) Higher energy spectrum coming from pre-equilibrium neutron emission.
3) Knock-on spectrum in the forward direction due to the direct process.
4) Only for ^{3}He and d projectiles, a broad bump in the forward spectrum produced from the breakup reaction of projectiles, (d,np) and (^{3}He,n2p) reactions.

The evaporation neutron spectrum of the thick target observed in the lab system, $\Phi(E,\theta)$, is given by

$$\Phi(E,\theta)=\int_{E_{th}}^{E_0} N\sigma_{nonel}(E_i)\frac{K}{2}\frac{\sqrt{E_\varepsilon}}{T^2}\exp\left(-\frac{\varepsilon}{T}\right)\left(\frac{dE_i}{dx}\right)^{-1}dE_i \quad (1)$$

(MeVSrprojectile)$^{-1}$,

where E_0 is the initial kinetic energy of the projectile in MeV; E_{th} is the threshold energy of the neutron-producing reaction in MeV; N is the atomic density of the target in atoms/cm^3; E_i is the projectile kinetic energy in the target in MeV; and dE_i/dx is the stopping power of the projectile in MeV/cm; ε is the neutron energy in the c.m. system in MeV; E is the neutron energy in the lab system in MeV; σ_{nonel} is the nonelastic cross section; K is the total number of evaporated neutrons per nonelastic collision; and T is the nuclear temperature in MeV.

When the target atomic mass M_t or the initial kinetic energy of the projectile E_0 is large, ε comes close to E. Therefore, $\Phi(E,\theta)$ in Eq. (1) becomes a function of E exp(-E/T) and $\Phi(E,\theta)/E$ indicates the exponential form exp(-E/T).

The neutron spectra emitted from the precompound nucleus state can also be expressed in the Maxwellian-type spectrum above the transition energy from equilibrium emission to pre-equilibrium emission. Differently from the evaporation process, however, the nuclear temperature, T', of a precompound nucleus in a pre-equilibrium state is dependent on the neutron emission angle θ. The neutron energy spectrum from the pre-equilibrium emission can be expressed as

$$\Phi(E,\theta)=K'\frac{E}{T'^2(\theta)}\exp\left(-\frac{E}{T'(\theta)}\right) \quad (2)$$

similarly as eq. (1). The T' value is higher than the nuclear temperature T of a compound nucleus in an equilibrium state and decreases with the emission angle, since the neutron emission from the hotter pre-equilibrium state occurs in a more forward direction.

Just for comparison, an analysis of a thin-target neutron energy spectrum is briefly described here which was published in refs. (7,8) The neutron production cross section differential in energy and angle, $d^2\sigma/dEd\Omega$, is peeled off into components, as

$$\frac{d^2\sigma}{dEd\Omega}=\sum_{i=1}^{n}A_i(E/T_i)\exp(-E/T_i), \quad (3)$$

where n=3 in ref.(7) and n=4 in ref.(8). This spectrum analysis is quite similar to our analysis for a thick-target neutron spectrum.

COMPARISON WITH EXPERIMENTAL RESULTS

As examples among of several experimental results, Figures 1 and 2 show the neutron energy spectra divided by energy, $\Phi(E,\theta)/E$, of copper target bombarded by 65 MeV α [9)] and of iron target by 710 MeV α [10)], respectively. In Fig.1, the neutron spectra are clearly divided into two components. The higher energy components are well fitted to Eq. (2) corresponding to the pre-equilibrium emission, whose nuclear temperature $T'(\theta)$ varies from 7.3 MeV at θ=0 deg to 3.5 MeV at θ=135 deg. The lower energy components show a good agreement with the evaporation spectrum of nuclear temperature T=2.1

with the evaporation spectrum of nuclear temperature T=2.1 MeV calculated from Eq.(1). While on the other hand, the neutron spectra in Fig. 2 are divided into three components. The lowest component corresponds to the evaporation spectrum and the other two belong to the pre-equilibrium neutron emission. The nuclear temperatures $T'(\theta)$ of the intermediate components are around 5-10 MeV and almost independent of θ, but the higher $T'(\theta)$ values are several tens of MeV and strongly dependent on θ.

In Figs. 1 and 2, the spectra show a broad bump from their exponential form in the forward direction. This bump spectra may come from the direct knockon process.

Fig. 3 shows the nuclear temperature of the evaporation component of the neutron spectrum as a function of initial projectile energy E_0. It increases with projectile energy and decreases with increasing target mass number, but does not depend so much on the type of projectile, and approaches a saturated value at about 100 MeV. For $T'(\theta)$, the data are too small to discuss their dependence on E_0 and target atomic number.

TOTAL NEUTRON YIELD

The total neutron yield can be obtained by integrating the neutron energy spectrum $\Phi(E,\theta)$ as

$$Y(E_0)= 2\pi\int_0^{\pi}\sin\theta\, d\theta\int_0^{E_0}\Phi(E,\theta)dE \quad , \tag{4}$$

but the experimental data on neutron spectrum are usually given in the energy region higher than a few MeV. Then, neutrons of energy lower than a few MeV can be approximated to be produced by the evaporation process having a Maxwellian energy distribution given by

$$\phi_n(E)=C\frac{E}{T^2}\exp(-E/T), \tag{5}$$

where T is the nuclear temperature and C is a normalization constant. The total yield of evaporation neutrons below certain energy, Ecut, can be given by

$$\begin{aligned} Y_{slow}(E_0) &= 2\pi\int_0^{\pi}\sin\theta\, d\theta\int_0^{E_{cut}}\frac{C}{T^2}E\exp\left(-\frac{E}{T}\right)dE \\ &= 4\pi\frac{C}{T}\left[T-(E_{cut}+T)\exp\left(-\frac{E_{cut}}{T}\right)\right] . \end{aligned} \tag{6}$$

The total neutron yields $Y(E_0)$ thus obtained are shown in Fig.4 as a function of projectile energy per nucleon in MeV/amu for various projectile and target combinations cited from two summarized papers[11),12)]. This figure indicates that the dependence of total neutron yield on the target atomic number becomes less for the heavier projectile and the total neutron yield increases with the increase of the projectile mass, excluding the deuteron beam which causes the stripping reaction. It is needed to have much more data on neutron production by various projectiles other than proton.

REFERENCES

1) T. Nakamura et al., At. Data Nucl. Data Tables 32 (1985) 471.
2) F. Clapier and C.S.Zaidins, Nucl. Instr. Meth. 217 (1983) 489.
3) T. Nakamura and Y.Uwamino, Phys. Rev. C29 (1984) 1317.
4) T. Nakamura, Nucl. Instr. Meth. A240 (1985) 207.
5) L.S. August et al., Phys. Med. Biol. 21 (1976) 931.
6) R. Madey, F.M. Waterman and A.R. Baldwin, Phys. Rev. C14 (1976) 801.
7) K. Tsukada and Y. Nakahara, Atomkernenergie-Kerntechnik 44 (1984) 186.
8) S. Pearlstein, Nucl. Sci. Eng. 95 (1987) 116.
9) K. Shin et al., Phys. Rev. C29 (1984) 1307.
10) R.A. Cecil et al., Phys. Rev. C21 (1980) 2471.
11) T. Nakamura, Genshikaku-Kenkyu 29 (1985) 55.
12) K. Tesch, Rad. Protection Dosimetry 11 (1985) 165.

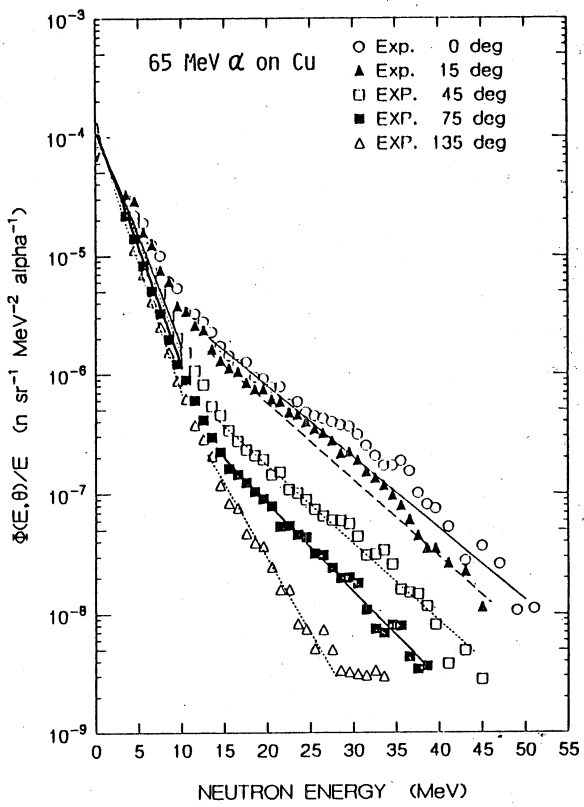

Fig.1 Analytical fitting of the measured neutron spectra divided by the neutron energy E of $\Phi(E, \theta)/E$ at emission angle θ from copper target by 65MeV alpha ion bombardment to two Maxwellian-type spectra.

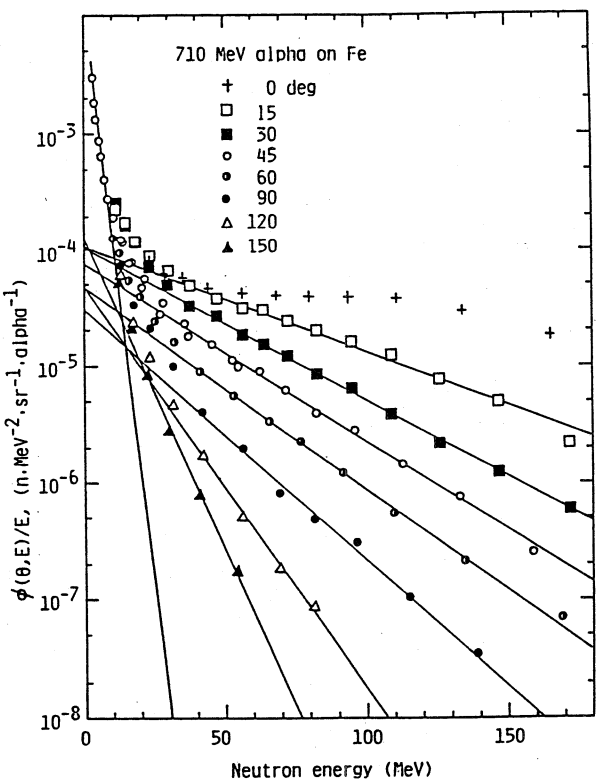

Fig.2 Analytical fitting of the measured neutron spectra $\Phi(E, \theta)/E$ from iron target by 710 MeV alpha ion bombardment to three Maxwellian-type spectra.

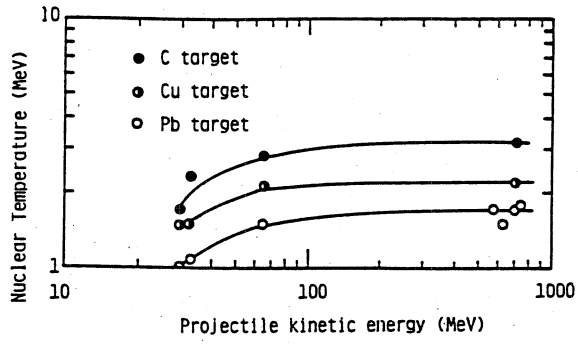

Fig.3 Dependence of the nuclear temperature T of the compound nucleus in an equilibrium state on the projectile kinetic energy Eø.

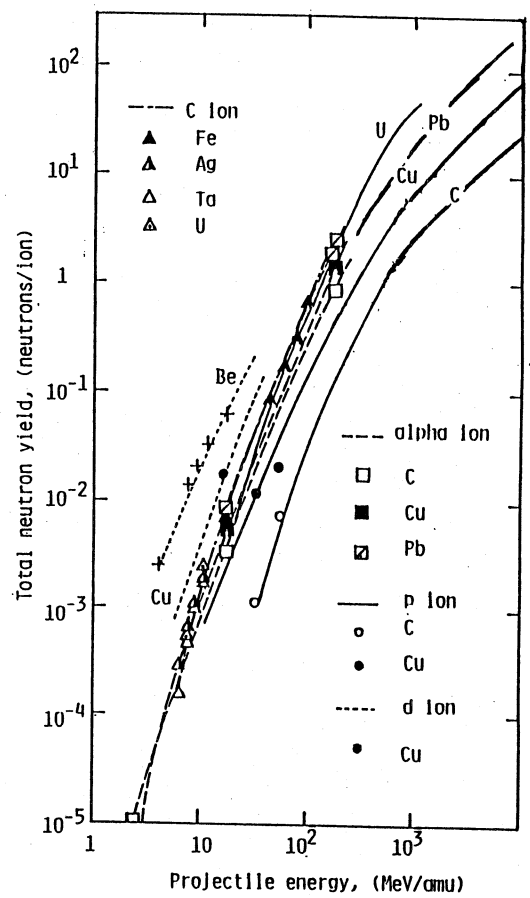

Fig.4 Total neutron yields per incident ion for various projectile-target combinations.